Discharge Characteristics of Ring Type Flow Stabilized Pulsed Corona Discharge Radical Shower Systems

V. Lakhian, F. Bocquet, D. Brocilo, G.D. Harvel, Jen-Shih Chang IEEE Senior Member, D. Ewing, M. Watanabe, H. Matsubara, H. Hirata and S. Matsumoto, P. Fanson.

***Abstract*— Discharge characteristics of a ring-type flow-stabilized pulsed corona discharge radical shower system (RCDRS) were investigated. A RCDRS with 6 hollow electrodes was studied, and a low dc voltage charging of an ignition coil type power supply was used to generate a pulse high voltage. Experiment were conducted for an applied charging dc voltage from 5V to 18V, a pulse repetition rate from 50 Hz to 200 Hz, and injected air flow rate from 2.5 to 4.6 L/min. per hollow electrode. The discharge characteristics were measured using current and voltage probes, and the morphology of the discharge was observed using a CCD camera. The pulsed waveforms of current, voltage and power (secondary side output) were studied in terms of the input power (primary side), as well as the current and voltage, with the observed optical images for optimization. The results show that the maximum discharge current, voltage and power increase with increasing primary side dc voltage or power. The pulse repetition rate affected the maximum discharge characteristics in terms of the primary side dc voltage, while the air flow rate did not. The maximum volume averaged plasma density is the order of 10^{11} ions / cm^3 for the 11cm in diameter and 5 cm long flow channel volume.**

***Index Terms*— pulsed corona, flow stabilized corona discharge, radical shower system.**

I. Introduction

Flow stabilized corona discharge radical shower systems have been developed to remove , NO_2 and SO_2 [1-5], or a combination of these pollutants [6,7] from exhaust gas flow, or to suppress diesel soot deposition from diesel exhaust flows [8]. The flow stabilized radical shower systems in these applications typically consist of pipes with a series hollow electrodes for the injected gas positioned in the main gas flow. A ring-type radical shower reactor with hollow electrodes in a pipe wall should serve to form a flow stabilized radical shower in the reactor without blockage.

The flow stabilized radical shower systems are typically powered using a high voltage dc, and ac/dc power supplies [6]. The radical shower systems can also be powered using a pulsed power supply that can operate from a low voltage power supply [8]. The pulsed systems are typically less efficient but make it possible to implement a flow stabilized radical shower where high voltage sources are not available.

The experiments reported in this paper were performed to characterize a ring-type flow-stabilized corona discharge radical shower system. The electrodes were in a cylindrical ring in a cylindrical pipe with the electrode for an electrohydrodynamic atomization electrode present in the center of the pipe [9]. The morphology of the plasma and the electrical discharge characteristics for the ring-type system operated with a pulsed power supply are presented herein.

II. Experimental Apparatus

Experiments were performed for a 6 hollow electrode ring-type corona discharge radical shower (RCDRS) system as shown in Fig. 1. The experimental apparatus consisted of a 120 mm diameter stainless steel reactor connected to a 120 mm diameter stainless steel pipe at a tee junction. The CDRS was an annular section with horizontal electrodes positioned 120 mm above the junction. The experiments were performed with an electrohydrodynamic atomization (EHDA) electrode positioned in the center of the reactor. The electrode was contained in a 25 mm diameter ceramic tube that was positioned in the middle of RCDRS as shown in Fig. 1. The EHDA electrode was 1.5 mm outer diameter tube that extended 10 mm beyond the ceramic case. The EHDA electrode was grounded in the experiments.

The main body of the CDRS was a Teflon annulus with an inner diameter of 100 mm and thickness of 50 mm. The system had 6 stainless steel hollow tube electrodes with inner diameters of 1.7 mm and outers diameters of 3.2 mm. The electrodes extended 10 mm inside the Teflon body, and extended approximately 25 mm outside of the Teflon body. The outer ends of the hollow electrodes were connected to plastic tubes from a common tube attached to a compressed air line. The air flow rate to the RCDRS was measured using a flow meter in the common tube.

Manuscript received April 17, 2009. This work was supported by the Toyota Motor Corporation.

V. Lakhian F. Bocquet, D. Brocilo, G.D. Harvel, J.S. Chang are/were with MACIRIS, McMaster University, Hamilton, ON Canada (V. Lakhian is corresponding author phone: 905-525-9140 ext. 24608 e-mail: lakhiavs@univmail.cis.mcmaster.ca). G. D. Harvel is also with the Faculty of Energy Systems and Nuclear Science, UOIT, Oshawa, Canada

D Ewing is with Dan W. Ewing, Toronto, On, Canada.

M. Watanabe, H. Matsubara, H. Hirata and S. Matsumoto are with TMC, Japan,

P. Fanson is with Toyota, USA.

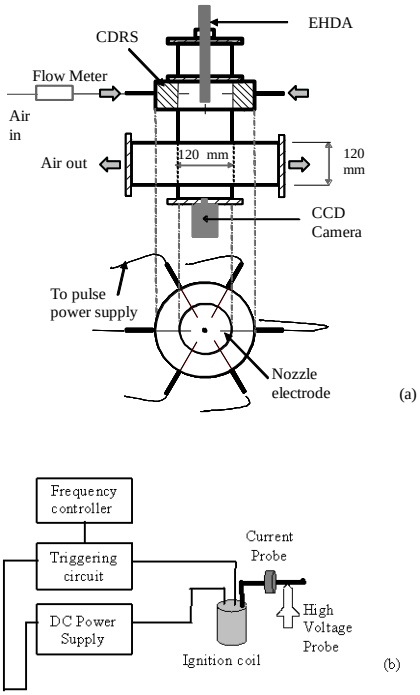

Fig. 1. Schematic of (a) the experimental apparatus used to characterize the RCDRS and (b) the pulse power supply.

The electrodes in the RCDRS were connected in parallel to a pulse power supply in Fig 1b which consisted of: a low-voltage primary dc power supply (0-18V), a frequency generator and controller that determined the discharge pulse repetition rate, and an ignition coil that produced the high voltage pulse. The stainless steel reactor served as the ground for the RCDRS.

The primary side voltage and current were determined from meters on the power supply. The discharge voltage was measured with a high voltage probe, while the discharge current was measured using a current probe. The probes were connected to a high-speed oscilloscope that captured the signals and recorded them for further analysis. Images of the corona discharge were captured using a CCD camera positioned at the bottom of the facility. The images were filtered to reduce noise and then processed to enhance the image contrast.

III. Morphology of Discharge

The typical morphology of discharge from the 6 electrode ring type corona radial shower is shown in Fig. 2. The discharge was strongest near the tips of the electrode as shown in the filtered image of the discharge in Fig 2a. The image with constant adjustment to enhance the image shows evidence of a 6 lobed discharge with each lobe centered around one of the 6 electrodes. The results are reasonably symmetric as expected since all of the electrodes were connected to the pulsed power supply. The discharge was small in the center of the channel. This may be due in part to

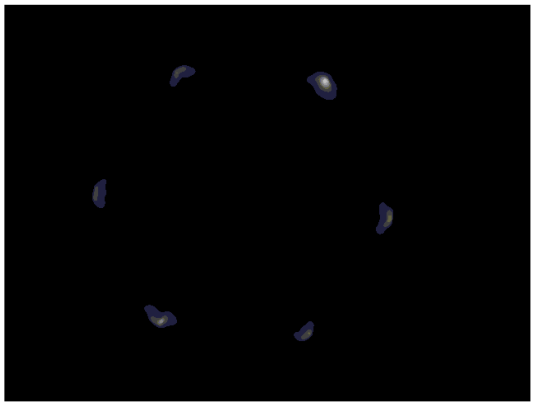

(a)

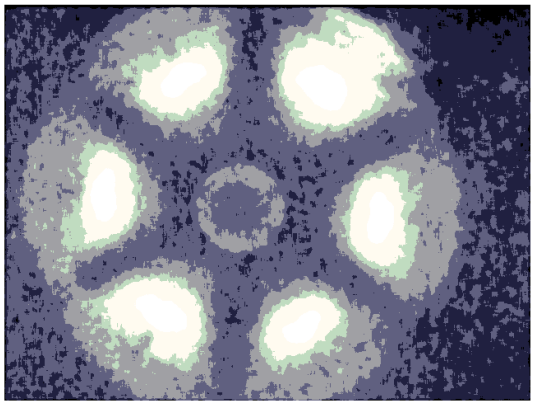

(b)

Fig. 2 Images of the corona for the 6 electrode ring-type CDRS system after (a) noise filterig and (b) contrast adjustment for a primary side charging voltage of 15.7V, flow per electrode of 4.6 L/min, and pulse repetition rate of 200 Hz.

the presence of the ceramic EHDA electrode holder in the center of the channel. The morphology of the discharges do not show a significant deformation on the edge closest to the channel center suggesting that the effect of EHDA electrode is small. Visualizations for different cases showed that the air flow rate did not have a significant impact on the observed corona discharge for flow rates per electrode 2.5 L/min to 4.6 L/min. The primary charging voltage and the pulse repetition rate did have an impact on the magnitude of the discharge though the basic morphology was similar with a six lobed discharge being observed in all cases.

IV. Discharge Characteristics and Plasma Parameter

Typical waveforms of the discharge voltage, discharge current, and discharge power are shown in Fig 3. The pulse duration is small relative to the duty cycle of the pulse. The rise time of the discharge voltage was approximately 50 μs. The discharge voltage was then constant for 100 μs during this primary pulse. The discharge current was in phase with the discharge voltage during the first half of the primary pulse, but decreases and becomes negative before the voltage. Much of the power in the discharge occurs in 100 μs. There are

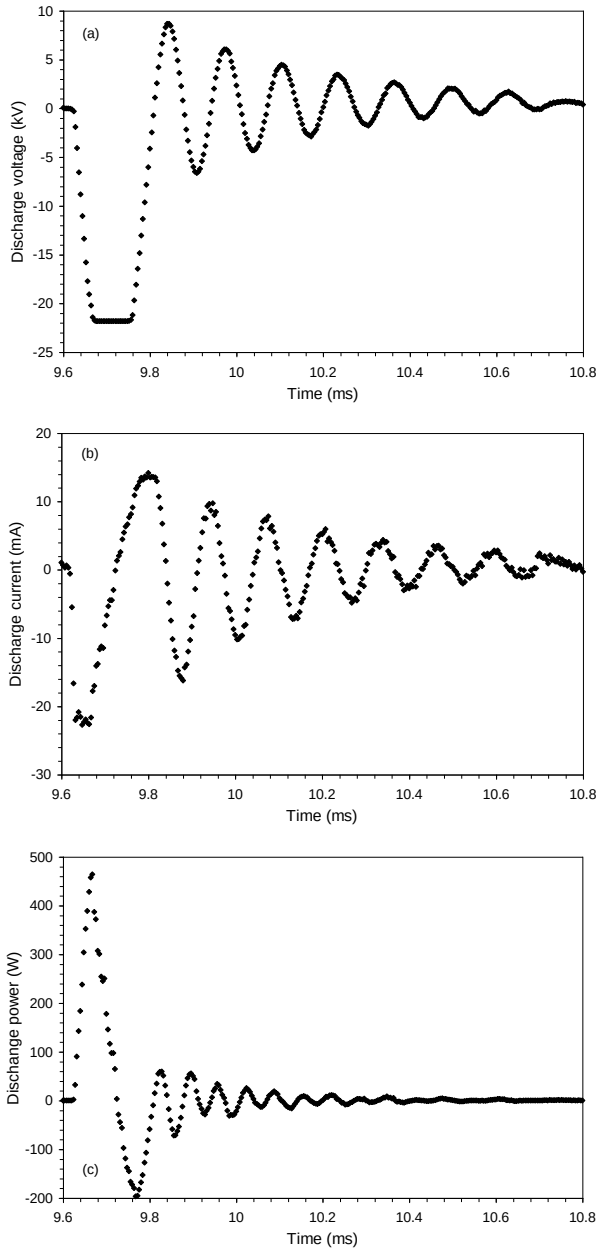

Fig 3. Typical waveforms of the (a) discharge voltage, (b) discharge current, and (c) discharge power from the 6 hollow electrode RCDRS for a primary side charging voltage of 15.7V, air flow rate per electrode of 4.6 L/min and a pulse repetition rate of 200Hz.

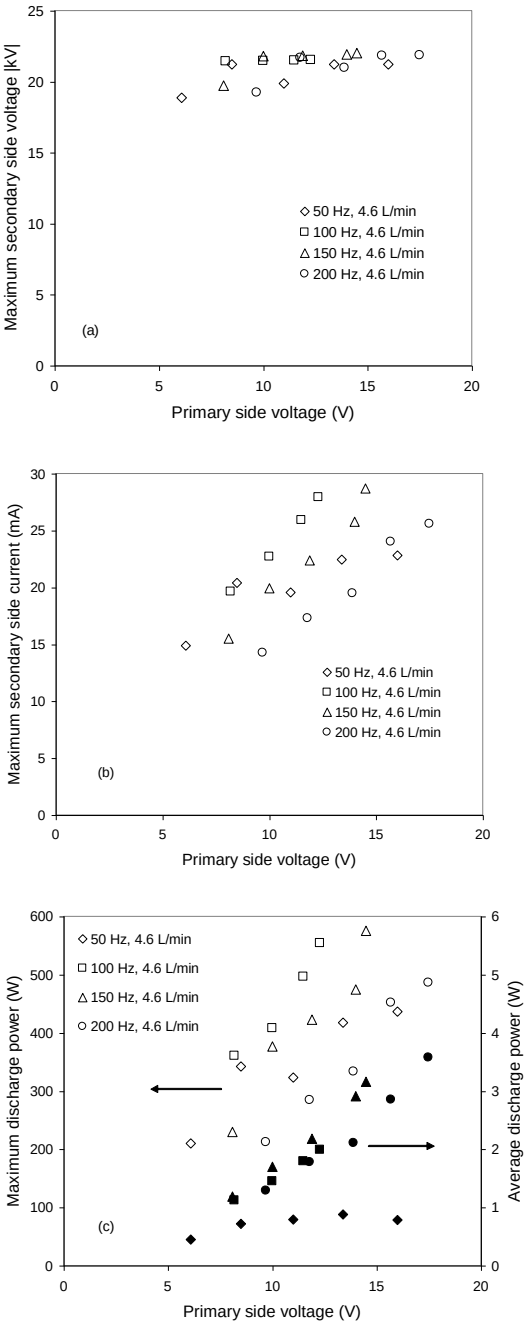

Fig 4. The change in (a) the maximum discharge voltage, (b) the maximum discharge current, and (c) the maximum and average discharge power as a function of the primary side voltage for pulse repetition rates of 50 to 200 Hz and an air flow rate per electrode of 4.6 L/min.

secondary pulses but the discharge power associated with these quickly decreases.

The effect of the pulse repetition rate on the change in the maximum discharge voltage and maximum discharge current as a function of the primary side charging voltage is shown in Fig. 4. The maximum discharge voltage initially increased with the primary side charging voltage before reaching a maximum charging voltage of approximately -21 kV. Thereafter, the maximum discharge voltage increased only slightly with the charging voltage. This plateau in the maximum charging voltage occurred at similar values for pulse repetition rates of 50 to 200 Hz. The primary charging voltage required to achieve this plateau increased with the pulse repetition rates and experiments at different flow rates showed this to be the case. The maximum discharge voltage for a given primary charging voltage decreased with the pulse repetition rate, particularly for repetition rates of 100 to 200 Hz. The maximum discharge power was largest for a pulse repetition rate of 100 Hz. The maximum discharge power shon in Fig 4c was lower at the pulse repetition rates of 150 and 200 Hz, though the average discharge power was similar for pulse

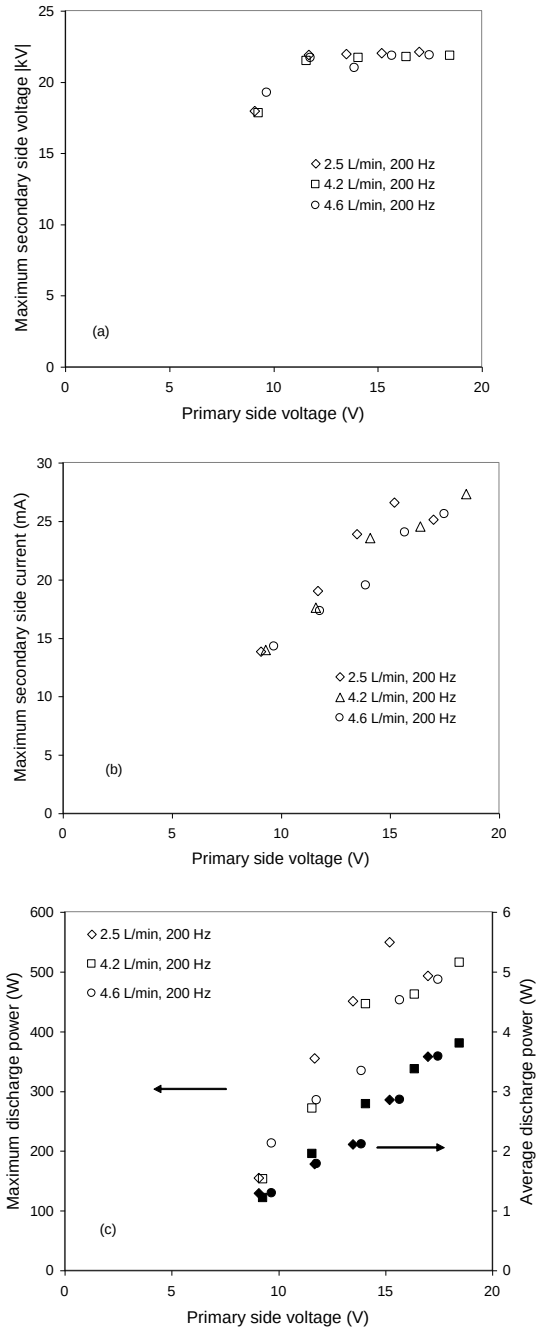

Fig 5. The change in (a) the maximum discharge voltage, (b) the maximum discharge current and (c) the maximum and average discharge power as a function of the primary side voltage for a pulse repetition rate of 200 Hz and air flow rates per electrode of 2.5 to 4.6 L/min.

repetition rates of 100 to 200 Hz, due to the increase in the number of pulses per second. The maximum discharge power for 50 Hz was lower than for 100 Hz, and the average discharge power was significantly lower than all the other cases. The average discharge power appears to decrease at 200 Hz, suggesting an optimal repetition rate of 100 to 200 Hz.

The effect of the air flow rate through the electrodes on the maximum discharge voltage, maximum discharge current, and discharge power is shown in Fig. 5. The air flow rate did not have a significant impact on the maximum discharge voltage for a given charging voltage for the pulse repetition rate of 200 Hz. The maximum discharge current and discharge power appear to increase modestly with the air flow rate. The results for the other repetition rate also showed modest changes in the discharge properties.

The volume average plasma density was estimated for the results here following [10]. The maximum volume averaged plasma density is on the order of 10^{11} ions / cm^3 based on the 10cm diameter and 5 cm long flow channel volume corresponding to the RCDRS section.

V. Concluding Remarks

Experiments were performed to characterize the discharge from a 6 electrode ring-type flow pulsed corona discharge radical shower system operated with a pulsed power supply. The ring-type system produced a lobed discharge with lobes corresponding to the electrodes. The maximum discharge voltage initially increased with the primary charging voltage, with a maximum discharge voltage of approximately -21 to -22 kV. The maximum discharge current and power increased with the primary charging voltage. The discharge depended on the pulse repetition rate, and with an optimal pulse repetition rate of 100 to 200 Hz. The discharge did not show a strong dependence on the mass flow rate per electrode. The maximum volume averaged plasma density is on the order of 10^{11} ions / cm^3 based on the 10cm diameter and 5 cm long flow channel volume

Acknowledgment

The authors would like to acknowledge M. Ibe, M. Ishkiriyama, C. Ayuralt, and M. Sun for valuable discssuion and comment. This work is supported by Toyota MC and TEMA.

References

[1] T. Ohkubo, S. Kanazawa, Y. Nomoto, J.-S. Chang, and T. Adachi, "Time dependence of NO_x removal rate by a corona radical shower system", *IEEE Transactions on Industry Applications*, vol. 32(5), pp. 1058-1062, September/October 1996.

[2] J. Y. Park, I. Tomicic, G. F. Round, and J.-S. Chang, "Simultaneous removal of NO_x and SO_2 from NO-SO_2-N_2-O_2 gas mixtures by corona radical shower systems", *Journal of Physics D: Applied Physics*, vol. 32, pp. 1006-1011, 1999.

[3] J.-S. Change, K. Urashima, Y.X. Tong, W.P. Liu, H.Y. Wei, F.M. Yang, and X.J. Liu, "Simultaneous removal of NO_x and SO_2 from coal boiler flue gases by DC corona shower systems: pilot plant tests", *Journal of Electrostatics*, vol 57, pp. 313-323, 2003.

[4] J. Li, M. Sun, Y. Wu, K. Shang, N. Wang and G. Li, Experimental investigation on activating water vapor and ammonia by dc corona radical shower technology for removal of SO2 from flue gases, J. Adv. Oxidation tech., vol. 7 (2) , pp. 146-153. 2004.

[5] K. Yukimura, K. Kawamura, S. Kanmbara , H. Morutomi and T. Yamashita, Correlation of energy efficiency of NO removal by inttermittend DBD radical injection methodes, IEEE Trans. Plasma Sci., vol. 33, pp. 763-770, 2005.

[6] J.-S. Chang, "Recent development of plasma pollution control technology: a critical review" *Science and Technology of Advanced Materials*, vol 2, pp. 571-576.

[7] R. Hakam and H. Akiyama, "Air pollution control by electrical discharge" *IEEE Transactions on Dielectrics and Electric Insulation*, vol 7(5), pp. 634-683, 2000.

[8] J.S. Chang , C. Luthereau, E. dela Cruze, P.I. Khalaf, D. Borocilo, G.D. Harvel, D. Ewing, N.A. Debacher, F. McCluskey, J.S. Cotton and M.

Bardeleben. “Plasma suppression of diesel soot deposition during diesel engine operations”, *International Journal of Plasma Environment Science and Technology* vol 3(1), March 2009.

[9] J.S. Chang, C. Ayault, D. Brocilo, D. Ewing, G. D. Harvel, K. Urashima, H. Hirata, S. Matsumoto, P. Fanson, “Electrohydrodymic atomization two-phase flow regime map for liquid hydrocarbon under pulsed electric fields with co-gas flow”, *Journal of Electrostatics*, vol.

[10] J.S. Chang “Physics and chemistry of plasma pollution control technology”, *Plasma Sources Science and Technology*, vol 17, pp. 1-6, 2008.